Adding salt to an aqueous solution of *t*-butanol: Is hydrophobic association enhanced or reduced?

Dietmar Paschek[a)] and Alfons Geiger
Physikalische Chemie, Universität Dortmund, D-44227 Dortmund, Germany

Momo Jeufack Hervé and Dieter Suter
Fachbereich Physik, Universität Dortmund, D-44227 Dortmund, Germany

Recent neutron scattering experiments on aqueous salt solutions of amphiphilic *t*-butanol by Bowron and Finney [Phys. Rev. Lett. **89**, 215508 (2002); J. Chem. Phys. **118**, 8357 (2003)] suggest the formation of *t*-butanol pairs, bridged by a chloride ion via $O-H\cdots Cl^-$ hydrogen bonds, leading to a reduced number of intermolecular hydrophobic butanol-butanol contacts. Here we present a joint experimental/theoretical study on the same system, using a combination of molecular dynamics (MD) simulations and nuclear magnetic relaxation measurements. Both MD simulation and experiment clearly support the more classical scenario of an enhanced number of hydrophobic contacts in the presence of salt, as it would be expected for purely hydrophobic solutes. [T. Ghosh *et al.*, J. Phys. Chem. B **107**, 612 (2003)]. Although our conclusions arrive at a structurally completely distinct scenario, the molecular dynamics simulation results are within the experimental error bars of the Bowron and Finney data. © *2006 American Institute of Physics.* [DOI: 10.1063/1.2188398]

I. INTRODUCTION

Nonpolar solutes, such as noble gases or alkanes, do not like to be dissolved in water. Consequently, they are considered as "hydrophobic" and their corresponding solvation free energy is found to be large and positive.[1–5] This effect is typically found to be significantly strengthened when salt is added, leading to a further reduced solubility of hydrophobic species such as noble gases or methane.[6,7] The increasing excess chemical potential is usually found to be proportional to the salt concentration over large concentration ranges and is therefore parametrized in terms of Setschenow's concentration independent salting out coefficient.[6] In line with the observation of an increased positive solvation free energy upon addition of salt, Ghosh *et al.*[8] reported an increased number of hydrophobic contacts in a diluted aqueous solution of methane. Moreover, for the case of hydrophobic interactions in a hydrophobic polymer chain, an approximately linear relationship between the salt concentration and the strength of pairwise hydrophobic interactions has been determined.[9] This observation seems to be in line with the finding of Widom *et al.*[5] and Koga[10] that the excess chemical potential of a small hydrophobic particle and the strength of hydrophobic pair interactions appears to be (almost) linearly related.

However, purely hydrophobic compounds are probably not very typical representatives of biophysical constituents. Usually, proteins and membrane-forming lipids are amphiphilic in the sense that they are composed of both, hydrophobic and hydrophilic groups, where the latter ones ensure

a sufficiently high solubility in an aqueous environment. In addition, the delicate interplay between hydrophobicity and hydrophilicity is exploited by nature to control the dimensions of molecular aggregates in aqueous solution.[11–14] Small amphiphilic alcohols might thus be considered as a minimalist model system to explore the subtle interplay between hydrophobic and hydrophilic effects. Numerous experimental studies on alcohol aggregation in aqueous solution have been reported, based on nuclear magnetic resonance[15–19] as well as light-, x-ray-, and neutron scattering techniques.[20–26]

Salts are known to influence a number of properties of aqueous solutions in a systematic way.[27] The effect of different anions and cations appears to be ordered in a sequence, already proposed by Hofmeister in 1888,[28] deduced from a series of experiments on the salt's ability to precipitate "hen-egg white protein." However, the exact reason for the observed specific cation and anion sequences is still not completely understood, since the same salt that can precipitate a protein at one concentration can "salt it in" at another.[29] Model calculations[30] as well as nuclear magnetic relaxation experiments[16] propose a delicate balance between ion adsorption and exclusion at the solute interface, tuned by the solvent (water) structure modification according to the ion hydration[31,32] and hence possibly subject to molecular details.

Recently, Bowron and Finney[23,26] provided a detailed mechanistic picture of the possible salting out process of *t*-butanol (TBA) in aqueous solution. The atomistic structure of the solution was determined from neutron scattering experiments, varying solute and solvent isotopic compositions.[33] However, their analysis relies largely on the accuracy of the employed empirical potential structure refinement (EPSR) technique of Soper.[34,35] Their main obser-

---

[a)]Author to whom correspondence should be address. FAX: +49-231-755-3937. URL: http://ganter.chemie.uni-dortmund.de/~pas . Electronic mail: dietmar.paschek@udo.edu

vation is that TBA molecules form dimers that are connected by hydrogen bonds to a central chloride anion. Salting out appears hence due to solute aggregates, which are formed by anion bridges between the hydroxyl groups, increasing the solutes' overall hydrophobic surface and thus reducing the solubility of the whole complex.[36–38] A straightforward conjecture would suggest that the salting out of proteins could be driven by analogous anion-bridged aggregates. We would like to point out that the proposed mechanism has similarity with the "differential hydrophobicity" concept of Burke *et al.*[39] used to explain the specific protein-aggregation behavior observed in Huntington's disease.

The molecular dynamics simulations discussed here, however, do not show any evidence for a "salting out" scenario, as proposed by Bowron and Finney. Instead, upon addition of salt we find an increased number of hydrophobic contacts of the TBA molecules which increases with higher salt concentration. Using a combination of molecular dynamics simulations and nuclear magnetic relaxation experiments we show that an association parameter based on NMR measurable quantities and introduced by Hertz[40] and Hertz and Tutsch[41] is a useful measure for the association of TBA molecules in the present case. Both simulation and NMR experiments consistently support the classical picture of an enhancing hydrophobic association in the case of aqueous TBA/salt solutions.

II. METHODS

A. Dipolar nuclear magnetic relaxation and correlations in the structure and dynamics of aqueous solutions

The molecular dynamics simulations yield the time-dependent positions of the atomic nuclei. Experimentally, the individual molecular positions are not available. However, a useful measure of molecular association is experimentally accessible via the measurement of nuclear spin relaxation rates and is discussed in a separate section below. In this section we would like to briefly summarize the underlying theory.

The most important contribution to the relaxation rate of nuclear spins with $I = 1/2$ is the magnetic dipole-dipole interaction. The relaxation rate, i.e., the rate at which the nuclear spin system approaches thermal equilibrium, is determined by the time dependence of the magnetic dipole-dipole coupling. For like spins, it is[42]

$$T_1^{-1} = 2\gamma^4\hbar^2 I(I+1)(\mu_0/4\pi)^2$$
$$\times \left\{ \int_0^\infty \left\langle \sum_j^N \frac{D_{0,1}[\Omega_{ij}(0)]}{r_{ij}^3(0)} \frac{D_{0,1}[\Omega_{ij}(t)]}{r_{ij}^3(t)} \right\rangle e^{i\omega t} dt \right.$$
$$\left. + 4\int_0^\infty \left\langle \sum_j^N \frac{D_{0,2}[\Omega_{ij}(0)]}{r_{ij}^3(0)} \frac{D_{0,2}[\Omega_{ij}(t)]}{r_{ij}^3(t)} \right\rangle e^{i2\omega t} dt \right\},$$
(1)

where $D_{k,m}[\Omega]$ is the k,m-Wigner rotation matrix element of rank 2. The Eulerian angles $\Omega(0)$ and $\Omega(t)$ at time zero and time t specify the dipole-dipole vector relative to the laboratory fixed frame of a pair of spins, r_{ij} denotes their separation

distance, and μ_0 is the permittivity of free space. The sum indicates the summation of all j-interacting-like spins in the entire system. $\langle \cdots \rangle$ denotes averaging over all equivalent nuclei i and all time zeros. For the case of an isotropic fluid and in the extreme narrowing limit Eq. (1) simplifies to[43]

$$T_1^{-1} = 2\gamma^4\hbar^2 I(I+1)\left(\frac{\mu_0}{4\pi}\right)^2 \int_0^\infty G_2(t)dt.$$
(2)

The dipole-dipole correlation function here is abbreviated as $G_2(t)$ and is available through[43,44]

$$G_2(t) = \left\langle \sum_j r_{ij}^{-3}(0) r_{ij}^{-3}(t) P_2[\cos\theta_{ij}(t)] \right\rangle,$$
(3)

where $\theta_{ij}(t)$ is the angle between the vectors $\mathbf{r}_{ij}$ joining spins i and j at time 0 and at time t (Ref. 43) and P_2 is the second Legendre polynomial.

To calculate the integral, the correlation function $G_2(t)$ can be separated into an r^{-6} prefactor, which is sensitive to the structure of the liquid (average internuclear distances) and a correlation time τ_2, which is obtained as the time integral of the normalized correlation function $\hat{G}_2(t)$, and which is sensitive to the mobility of the molecules in the liquid,

$$\int_0^\infty G_2(t)dt = \left\langle \sum_j r_{ij}^{-6}(0) \right\rangle \tau_2.$$
(4)

From the molecular dynamics (MD)-simulation trajectory data the correlation function G_2 and hence T_1 can be calculated directly. From the definition of the dipole-dipole correlation function in Eq. (3) it follows that the relaxation time T_1 is affected by both reorientational and translational motions in the liquid. Moreover, it is obvious that it also depends strongly on the average distance between the spins and is hence sensitive to changing inter- and intramolecular pair distribution functions.[40,41] In addition, the r^{-6} weighting introduces a particular sensitivity to changes occurring at short distances. For convenience, one may divide the spins j into different classes according to whether they belong to the same molecule as spin i, or not, thus arriving at an *inter*- and *intramolecular* contribution to the relaxation rate

$$T_1^{-1} = T_{1,\text{inter}}^{-1} + T_{1,\text{intra}}^{-1},$$
(5)

which are determined by corresponding intra- and intermolecular dipole-dipole correlation functions $G_{2,\text{intra}}$ and $G_{2,\text{inter}}$. The intramolecular contribution is basically due to molecular reorientations and conformational changes and has been used extensively to study the reorientational motions, such as that of the H–H vector in CH_3 groups in molecular liquids and crystals.[45] In the course of this paper, however, we are particularly interested in the association of solute molecules and will therefore focus on the intermolecular contribution (see also Sec. II D).

The structure of the liquid can be expressed in terms of the intermolecular site-site pair correlation function $g_{ij}(r)$, describing the probability of finding an atom of type j in a distance r from a reference site of type i according to[46]

$$g_{ij}(r) = \frac{1}{N_i \rho_j} \left\langle \sum_{k=1}^{N_i} \sum_{l=1}^{N_j} \delta(\mathbf{r} - \mathbf{r}_{kl}) \right\rangle, \tag{6}$$

where ρ_j is the number density of atoms of type j. The prefactor of the intermolecular dipole-dipole correlation function is hence related to the pair distribution function via an r^{-6} integral of the pair correlation function

$$\left\langle \sum_j r_{ij}^{-6}(0) \right\rangle = \rho_j \int_0^\infty r^{-6} g_{ij}(r) 4\pi r^2 dr. \tag{7}$$

Since the process of enhanced association in a molecular solution is equivalent with an increase of the nearest neighbor peak in the radial distribution function, Eq. (7) establishes a quantitative relationship between the degree of intermolecular association and the intermolecular dipolar nuclear magnetic relaxation rate.

B. Self-association: The Hertz *A* parameter

As a measure of the degree of intermolecular association, Hertz and co-workers[40,41,47] introduced a so-called association parameter A, which is a weighted integral of the pair correlation function of the nuclei contributing to the dipolar relaxation process (in the present case ^1H nuclei in TBA-$d1$ solutions) and is defined as[48]

$$A = \frac{1}{2} \frac{\gamma^4 \hbar^2}{a^4} \left(\frac{\mu_0}{4\pi}\right)^2 \int_0^\infty \left(\frac{a}{r}\right)^6 g_{HH}(r) 4\pi r^2 dr, \tag{8}$$

where a is the "closest approach distance of the interacting nuclei" and is usually assumed to be independent of the system's composition.[48]

The correlation time τ_2 of the intermolecular dipole-dipole interaction is approximated by[48]

$$\tau_{2,inter} = \frac{a^2}{3D}, \tag{9}$$

where D is the self-diffusion coefficient of the solute molecules. D can also be measured by NMR, using, e.g., pulsed field gradient experiments.[49]

Changes of the A parameter indicate short-range changes in the pair correlation function, which in the present study characterize the solvent-mediated interaction between the solute molecules. Enhanced association is identified by an increasing A parameter: As the first neighbor peak of $g_{HH}(r)$ becomes sharper, the A parameter increases.

Using the definitions of Eqs. (8) and (9), A is given in terms of NMR measurable quantities[48,50]

$$A = \frac{1}{T_{1,inter}} \frac{D}{\rho_H}, \tag{10}$$

where ρ_H is the number density of the ^1H nuclei in the system. Note that in our study ρ_H is kept nearly constant, varying only the additional salt content, whereas in most NMR studies[15–19,48,50] the concentration of the molecules, whose aggregation behavior is studied, is varied.[18]

Besides detecting $T_{1,inter}$ and D by NMR, we can also calculate these quantities, which are required for A, independently from our simulations and determine the A parameter

for our model system exactly the same way as it is done from the experiment. Since the TBA-TBA pair correlation function and the corresponding coordination number are also available from MD, the simulations thus provide a "proof of concept" for a system behaving closely similar to the real system.

C. MD-simulation details

We employ MD simulations in the *NPT* ensemble using the Nosé-Hoover thermostat[51,52] and the Parrinello-Rahman barostat[53,54] with coupling times $\tau_T = 1.5$ ps and $\tau_p = 2.5$ ps (assuming the isothermal compressibility to be $\chi_T = 4.5 \times 10^{-5}$ bar^{-1}), respectively. The electrostatic interactions are treated in the "full potential" approach by the smooth particle mesh Ewald summation[55] with a real space cutoff of 0.9 nm and a mesh spacing of approximately 0.12 nm and fourth order interpolation. The Ewald convergence factor α was set to 3.38 nm^{-1} (corresponding to a relative accuracy of the Ewald sum of 10^{-5}). A 2.0 fs time step was used for all simulations and the solvent constraints were solved using the SETTLE procedure,[56] while the SHAKE method was used to constrain the solute bond lengths.[57] All simulations reported here were carried out using the GROMACS 3.2 program.[58,59] The MOSCITO suit of programs[60] was employed to generate start configurations and topology files and was used for the entire data analysis presented in this paper. Statistical errors in the analysis were computed using the method of Flyvbjerg and Petersen.[61] For all reported systems initial equilibration runs of 1 ns length were performed using the weak coupling scheme for pressure and temperature control of Berendsen *et al.* ($\tau_T = \tau_p = 0.5$ ps).[62]

As in Refs. 25 and 26 we study 0.02 mole fraction aqueous solutions of *t*-butanol with and without the presence of sodium chloride. The simulations were carried out for 1 bar and 298 K. Our model system contains 1000 water molecules, represented by the three center extended simple point charge (SPC/E) model.[63] The flexible OPLS (optimized potentials for liquid simulations) all-atom force field[64] is employed for the 20 TBA molecules.

Here the bond lengths were kept fixed. Ten and twenty sodium chloride ion pairs were used to represent the salt solution. In order to check the influence of ion parameter variation, the two different parameter sets according to Heinzinger[65] and Koneshan *et al.*[66] were employed. All nonbonded interaction parameters are summarized in Table I. To ensure proper sampling and to allow an accurate determination of the system's structural and dynamical properties, the aqueous TBA solutions were studied for 50 ns, whereas the salt solutions were monitored for 100 ns. The performed simulation runs and resulting concentrations are indicated in Table II. For comparison, a pure water system of 500 SPC/E water molecules was simulated for 20 ns for the same conditions.

D. Experimental details

To experimentally determine the association behavior of TBA molecules in aqueous solutions we measured the inter-

TABLE I. Nonbonded interaction parameters used in the present study. The [1] refers to the ion parameter set of Heinzinger (Ref. [65]) whereas the [2] refers to the parameters of Koneshan *et al.* (Ref. [66]). Lorentz-Berthelot mixing rules according to $\sigma_{ij} = (\sigma_{ii} + \sigma_{jj})/2$ and $\epsilon_{ij} = \sqrt{\epsilon_{ii}\epsilon_{jj}}$ were employed.

Site	$q/|e|$	σ (nm)	ϵk^{-1} (K)
OW	−0.8476	3.1656	78.2
HW	+0.4238	⋯	⋯
CT	+0.265	3.50	33.2
CT(CH3)	−0.180	3.50	33.2
HC	+0.060	2.50	15.1
OH	−0.683	3.12	85.6
HO	+0.418	⋯	⋯
Na[1]	+1.0	2.73	43.06
Cl[1]	−1.0	4.86	20.21
Na[2]	+1.0	2.583	50.32
Cl[2]	−1.0	4.401	50.32

molecular NMR relaxation rates, self-diffusion coefficients, and the densities of the aqueous solutions. All experimental data are summarized in Table III.

The observed relaxation rates depend on inter- as well as intramolecular correlation functions. To extract the intermolecular rates, which are sensitive to the solute-solute association, we used the method of isotopic dilution.[67]

Since we are interested only in the hydrophobic methyl protons, we deuterated the water and the hydroxyl group of the TBA. Isotopic dilution was performed by mixing $(CD_3)_3COD$ (TBA-*d*10) with $(CH_3)_3COD$ (TBA-*d*1). We parametrize the dilution with the mole fraction

$$x_H = \frac{[\text{TBA-}d1]}{[\text{TBA-}d1] + [\text{TBA-}d10]}.$$

The basic assumption of the isotopic dilution procedure is that the relaxation rate is given by the sum of an intramolecular term, which is independent of the dilution, and an intermolecular term, which is proportional to the concentration of the corresponding molecular species. The contribution of the deuterated molecules can be taken as proportional to that of the protonated molecules, with a reduction factor[42]

$$\alpha = \frac{2}{3} \frac{\gamma_D^2}{\gamma_H^2} \frac{I_D(I_D + 1)}{I_H(I_H + 1)} = 0.042.$$

The observed relaxation rate becomes therefore

TABLE II. Parameters characterizing the performed MD-simulation runs. All simulations were carried out at $T = 298$ K and $P = 1$ bar. The star * indicates the simulation run employing the parameters of Koneshan *et al.* (Ref. [66]) for NaCl. For comparison a pure water simulation run of 500 SPC/E molecules over 20 ns was performed yielding an average density of 998.4 kg m^{-3}.

$N(H_2O)$	1000	1000	1000	1000
$N(TBA)$	20	20	20	20
$N(NaCl)$	⋯	10*	10	20
Simul. length τ (ns)	50	100	100	100
Density $\langle\rho\rangle$ (kg m^{-3})	991.5	1008.6	1002.6	1013.7
$\langle c(TBA)\rangle$ (mol l^{-1})	1.0170	1.0044	0.9984	0.9810
$\langle c(NaCl)\rangle$ (mol l^{-1})	⋯	0.5022	0.4992	0.9810

TABLE III. Experimental densities ρ, intermolecular relaxation times $T_{1,inter}$, and self-diffusion coefficients D for TBA-*d*1 in TBA-*d*1/D$_2$O/NaCl solutions. All experiments were carried out at $T = 298$ K at ambient pressure conditions. Also given are the TBA-*d*1 concentrations and the obtained A parameters.

TBA-*d*1:D$_2$O:NaCl	2:100:0	2:100:1	2:100:2
ρ (kg m^{-3})	1083.9	1106.1	1122.5
c(TBA) (mol l^{-1})	1.0059	0.9994	0.9882
c(NaCl) (mol l^{-1})	⋯	0.5270	1.0403
$T_{1,inter}$ (s)	44.89±1.74	41.02±4.73	37.92±0.13
D (10^{-9} m^2 s^{-1})	0.3962	0.3818	0.3792
A (10^{-39} m^5 s^{-2})	1.619	1.718	1.826

$$\frac{1}{T_1} = \frac{1}{T_{1,0}} + \frac{1}{T_{1,intra}} + \frac{1}{T_{1,inter}}[(1 - \alpha)x_H + \alpha]. \quad (11)$$

Here, $T_{1,intra}$ denotes the intramolecular contribution from protons within the methyl groups of the same molecule as the one being measured, $T_{1,inter}$ the intermolecular contributions between different TBA molecules, and $T_{1,0}$ all other terms, such as paramagnetic relaxation and interaction with other molecules such as D$_2$O. To extract the intermolecular term, we measured the relaxation rate as a function of the isotopic dilution and fitted the measured data points to Eq. (11).

The diffusion coefficients of TBA-*d*1 were determined from the pulsed gradient spin echo (PGSE) experiments,[49] where the gradient calibration was done using the diffusion coefficient of pure water.[68]

The ^{1}H number density in the TBA-*d*1/D$_2$O and TBA-*d*1/D$_2$O/NaCl solutions was obtained by measuring the mass density of the corresponding solutions with defined composition using a commercial Anton Paar oscillating U-tube density meter.

The TBA-*d*1 (99%) was purchased from Cambridge Isotope laboratories and the TBA-*d*10 (99%) from Isotec. The solvent D$_2$O with the purity of 99.96% was obtained from Merck KGaA. The solution was prepared by measuring the appropriate amount of each compound with a micropipette and by weighing a corresponding amount of NaCl. The degassing process was done by the usual freeze-pump-thaw technique, repeated several times until no gas bubbles develop from the solution. Finally, the samples were flame sealed. Relaxation and diffusion measurements were carried out at 600 MHz using a Varian Infinity spectrometer system. All experiments were conducted under controlled temperature conditions at 25 °C.

III. RESULTS AND DISCUSSION

A. Structural characterization of the aqueous TBA solutions

The most prominent feature of the combined neutron scattering/EPSR work of Bowron and Finney[23,26] is the observation of a significant decrease of the height of the first peak of the central carbon pair correlation function upon addition of sodium chloride. This decrease of the nearest
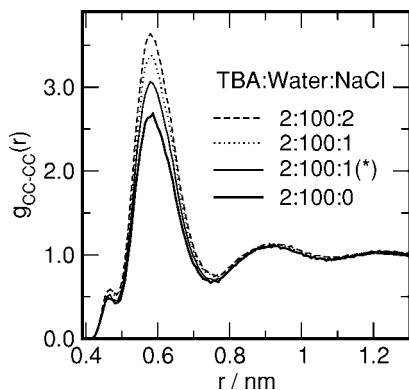
FIG. 1. Radial pair distribution functions between the TBA central carbon (CC) atoms in aqueous solutions at different salt concentrations. The star indicates the data belonging to the parameter set of Koneshan *et al.* (Ref. 66) for NaCl.

neighbor peak is accompanied by an increase of the second neighbor peak located at a distance of about 0.85 nm. From steric arguments and an analysis of their EPSR data, Bowron and Finney concluded that this process is according to the formation of chloride-bridged TBA pairs. In Fig. 1 we present the corresponding curves obtained from the present MD simulations. Surprisingly, exactly the opposite behavior is found. Upon addition of salt a notable increase of the first peak is observed, suggesting an enhanced TBA-TBA aggregation. Moreover, this increase is clearly more pronounced when increasing the salt concentration from about 0.5 M to about 1 M. Table IV provides a quantitative analysis of the pair correlation data in terms of coordination numbers

$$N_{\alpha\beta} = 4\pi\rho_\beta \int_{r_{min}}^{r_{max}} r^2 g_{\alpha\beta}(r) dr, \tag{12}$$

where ρ_β is the average number density of atom type β. In order to provide comparability with the data obtained by Bowron and Finney, the values of r_{min} and r_{max} for the distance intervals given in the upper part of Table IV were taken from Ref. 26. As the increasing peak height of the MD data suggests, the TBA-TBA coordination number increases with increasing salt concentration. Moreover, the increase is found to be significantly larger than the size of the associated error bars.

A more detailed picture of the structure of the aqueous salt solutions of TBA is given in terms of selected solute/solvent pair correlation functions in Fig. 2. To quantify the change of ion solvation with increasing salt concentration, ion/water-oxygen and ion/TBA-oxygen (first shell) coordination numbers are given the in lower part of Table IV. The changes in coordination numbers as the salt concentration doubles are only relatively small. However, apparently there is a certain tendency of the ions to slightly dehydrate, whereas the Na–OH coordination number is almost unchanged and the Cl–OH coordination slightly increases.

In order to take the amphiphilic nature of TBA more properly into account we also provide two-dimensional cylindrical pair correlation functions $g(z,r)$, indicating the arrangement of molecules around a central TBA molecule using the notation of[46]

TABLE IV. Coordination numbers for a 0.02 M aqueous solution of *t*-butanol (TBA) with and without added sodium chloride. The coordination numbers are obtained by integrating over the distance interval indicated. For a direct comparison, the values of Ref. 26 were taken for r_{min} and r_{max} for the upper part of the table. For the data shown in the lower part of the table (first shell coordination numbers) integration over $g(r)$ was performed to the first minimum of the ion-oxygen pair correlation function. CC refers to the central carbon atom of TBA. OW denotes the water oxygen, while OH specifies the oxygen atom in the hydroxyl group. The star indicates the parameter set for NaCl according to Koneshan *et al.* (Ref. 66). The neutron scattering data were taken from Ref. 26.

| Atom pair	r_{min} (nm)	r_{max} (nm)	2:100:0		2:100:1			2:100:2
			n scatt.	MD sim.	*n* scatt.	MD sim.	MD sim.*	MD sim.
CC–CC	0.43	0.75	1.5±0.7	1.15±0.01	0.8±0.5	1.32±0.05	1.27±0.01	1.45±0.03
CC–CC	0.75	1.00	1.0±0.6	1.41±0.02	1.8±0.8	1.39±0.06	1.39±0.02	1.40±0.04
OH–OH	0.25	0.35	0.02±0.08	0.042±0.001	…	0.047±0.002	0.043±0.002	0.048±0.001
OH–OW	0.25	0.35	2.5±0.6	3.017±0.002	2.4±0.6	2.975±0.005	2.992±0.002	2.950±0.002
Na–OW	0.21	0.30	…	…	4.2±1.1	5.562±0.004	5.582±0.003	5.454±0.002
Cl–OW	0.28	0.36	…	…	4.9±1.3	5.715±0.003	6.319±0.003	5.629±0.002
OH–Na	0.32	0.55	…	…	0.2±0.2	0.098±0.001	0.101±0.001	0.191±0.002
OH–Cl	0.29	0.38	…	…	0.2±0.2	0.0120±0.0002	0.0134±0.0003	0.0251±0.0004
HO–Cl	0.19	0.32	…	…	0.04±0.07	0.0135±0.0003	0.0141±0.0003	0.0279±0.0004
Na–OH	0.0	0.32	…	…		0.0307±0.0008		0.0304±0.0008
Cl–OH	0.0	0.39	…	…		0.0262±0.0005		0.0275±0.0004
Na–OW	0.0	0.32	…	…		5.780±0.004		5.669±0.002
Cl–OW	0.0	0.39	…	…		6.989±0.003		6.940±0.002
OH–Na	0.0	0.32	…	…		0.0154±0.0008		0.0304±0.0008
OH–Cl	0.0	0.39	…	…		0.0131±0.0005		0.0275±0.0004
OW–Na	0.0	0.32	…	…		0.0578±0.00005		0.1134±0.00003
OW–Cl	0.0	0.39	…	…		0.0699±0.00003		0.1388±0.00004
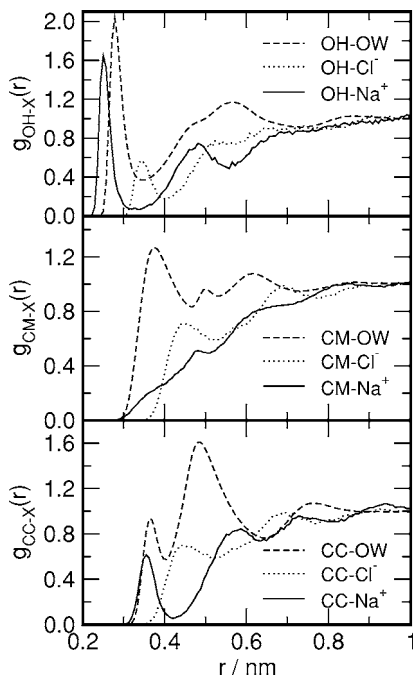
FIG. 2. Several representative TBA-solvent pair atom-atom radial distribution functions obtained from the TBA:water:NaCl 2:100:1 solution. CC denotes the TBA central carbon atom, whereas CM and OH specify the methyl-carbon and hydroxyl oxygens, respectively.

$$g(r,z) = \frac{1}{N_{TBA}\rho_\beta}\left\langle \sum_{i=1}^{N_{TBA}} \sum_{j=1}^{N_\beta} \delta(z - \mathbf{n}_{OH}\mathbf{r}_{ij}) \right.$$

$$\left. \times \delta(r - \sqrt{r_{ij}^2 - (\mathbf{n}_{OH}\mathbf{r}_{ij})^2}) \right\rangle, \tag{13}$$

where the z axis is aligned along the TBA intramolecular unit vector $\mathbf{n}_{OH} = \mathbf{r}_{OH}/r_{OH}$ pointing from the center of mass to the hydroxyl oxygen. The index i runs over all TBA molecules, whereas the index j runs over a particular subset of molecules (TBA, anions, or cations). The vector $\mathbf{r}_{ij} = \mathbf{r}_j - \mathbf{r}_i$ represents the center of mass separation between particles i and j. The schematic shown in Fig. 3 illustrates how the param-
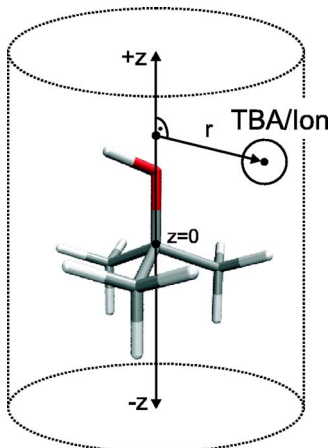

FIG. 3. Schematic illustration of the two-dimensional cylindrical pair distribution functions. Distribution of TBA and the ions around a central TBA molecule. The center of mass of the central TBA molecules is at ($z=0$, $r=0$) and the C–O bond is aligned along the z axis.

eters r and z are defined. The two-dimensional (2D) distribution of TBA molecules around a central TBA molecule is shown in Fig. 4. The radial pair distribution functions in Fig. 1 and the 2D distributions in Fig. 4 are interrelated and the radial distribution functions can be obtained by averaging over angles $\theta = \arctan(r/z)$. Figure 4 reveals that the prepeak in the CC–CC radial pair distribution function located at about 0.47 nm is due to hydrogen bonded TBA-TBA pairs. These pairs are identified by a separate dark spot at about $r = 0.3$ nm and $z = 0.35$ nm in close proximity to the hydroxyl group in Figs. 4(a) and 4(b). As deduced from the radial distribution functions in Fig. 1, the addition of salt leads to an increased aggregation of TBA. The difference between the two-dimensional distribution functions with and without salt, shown in Fig. 4(c), reveals that aggregation occurs predominantly on the methyl-group side of the TBA molecule: The region with negative z shows an increase in peak height of about 0.5, whereas on the hydrophilic side, the peak heights remain almost unchanged.

The distributions of the ions around a TBA molecule are shown in Fig. 5. Dark regions close to the hydroxyl group indicate a significant stability of TBA-ion complexes. A remarkable difference is observed for adsorption of the different ions at the aliphatic side of TBA. The chloride ions tend to adsorb close to the methyl groups and are present as a gray shadow on the hydrophobic side of the TBA molecule, as shown in Fig. 5(b), whereas the sodium completely tends to avoid that region. Consequently, there is practically no peak in the methyl-carbon-sodium radial pair correlation function in Fig. 2. This observation seems to be in line with the recently reported preferential anion adsorption at the liquid-gas interface,[69–71] which has structural similarities with the interface to a hydrophobic surface.[11,72,73] The tendency of the chloride ion to attach to the methyl groups might also explain the observed slight increase in the Cl–OH coordination number. A chloride ion just gets more frequently attached to the OH group since due to the preferential methyl-group-chloride interaction the chloride sees a higher local TBA concentration.

Finally, in order to prove whether there is a significant amount of chloride-bridged TBA-TBA configurations we calculate the two-dimensional cylindrical $(TBA-Cl^-)\cdots TBA$ correlation functions of a second TBA molecule around a TBA$-$Cl$^-$ contact pair with a center of mass distance less than 0.64 nm according to

$$g(r,z) = \frac{1}{N_{TBA-Cl}\rho_{TBA}}$$

$$\times \left\langle \sum_{i=1}^{N_{TBA-Cl}} \sum_{j=1}^{N_{TBA}} \delta(z - \mathbf{n}_{TBA-Cl}\mathbf{r}_{ij}) \right.$$

$$\left. \times \delta(r - \sqrt{r_{ij}^2 - (\mathbf{n}_{TBA-Cl}\mathbf{r}_{ij})^2}) \right\rangle. \tag{14}$$

Here $\mathbf{n}_{TBA-Cl}$ is the unit vector describing the orientation of a TBA$-$Cl$^-$ contact pair. An illustration is given in Fig. 6. As can be seen clearly from Fig. 7, the vast amount of TBA molecules is located on the TBA side of the TBA$-$Cl$^-$ pair,
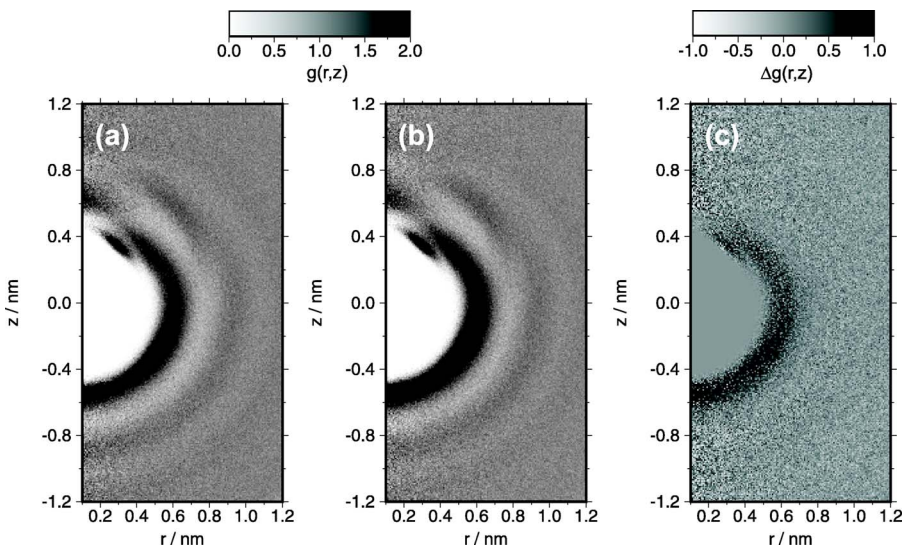
FIG. 4. Two-dimensional cylindrical center of mass pair distribution functions $g(r,z)$ of TBA around a central TBA molecule with the C–O vector pointing upwards. (a) 2 TBA: 100 water. (b) 2 TBA: 100 water: 1 NaCl; (c) Difference between the distribution functions shown in (b) and (a) (salt minus no salt).

practically ruling out a significant contribution of TBA−Cl⁻−TBA bridges.

As the two-dimensional cylindrical pair distribution functions indicate, the MD simulations furnish a scenario of an increased number of hydrophobic contacts in an aqueous solution of TBA in the presence of sodium chloride, in contrast to the observations of Bowron and Finney. However, when taking a look at the published data and considering the given size of error bars, the *n*-scattering and MD simulation are not at all contradictory. A quantitative comparison of the obtained coordination numbers is given in Table IV. Almost all indicated values agree within the given errors or are at least very close to each other. In fact, the large error in the *n*-scattering data for the central carbon (CC) coordination numbers for the first and second hydration shells probably forbids a clear distinction between both scenarios just relying

on the *n*-scattering data. In fact, only about 0.04% of the scattering functions considered in Ref. 26 is due to contributions from the CC pair correlation functions $g_{CC-CC}(r)$.

Very recently Lee and van der Vegt have published a series of molecular dynamics simulations of TBA/water mixtures with varying composition.[74] In their study, using the SPC model[75] for water, they found the original united-atom OPLS potential[76] for TBA less satisfactory and hence derived an improved set of model parameters for tertiary butanol, basically by adjusting the charges on the OH group. Lee and van der Vegt reported a too strong association of the TBA molecules for the original united-atom OPLS model. We would like to point out that the reported effect might be also partly attributed to the use of the SPC water model, since an analogous solvent-model dependence has been recently observed for simple solutes (noble gases). Paschek[77] found for the SPC model a substantially stronger hydrophobic association, which experiences also a significantly smaller temperature dependence. For our present study we choose the SPC/E model on purpose, since it reproduces sev-
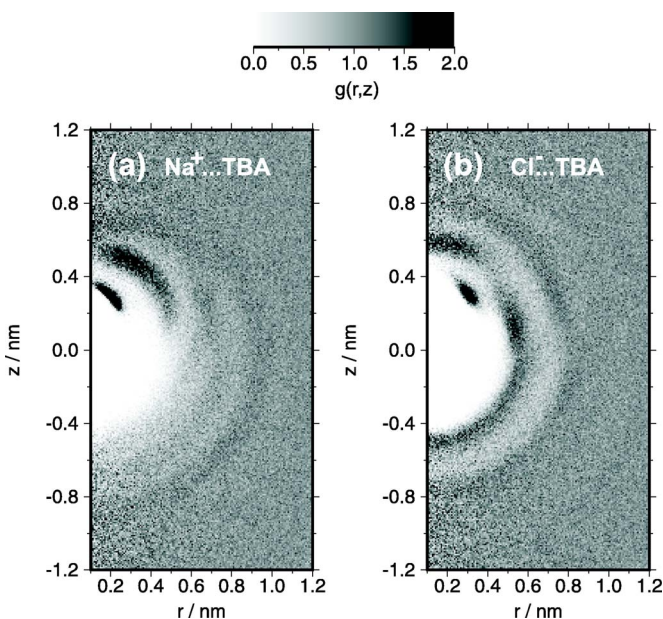

FIG. 5. Two-dimensional cylindrical pair distribution functions $g(r,z)$ of the sodium (a) and chloride (b) ions around a central TBA molecule with the C–O vector pointing upwards. From the simulation with composition TBA:water:NaCl of 2:100:1.
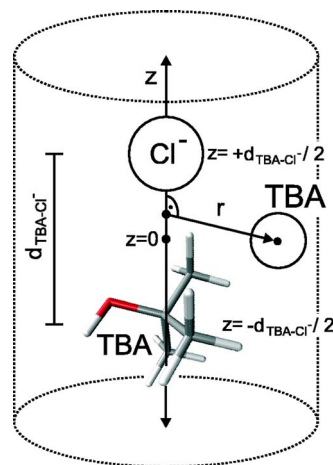

FIG. 6. Schematic illustration of the two-dimensional cylindrical pair distribution function $g(r,z)$ of TBA molecules around a TBA−Cl⁻ contact pair with $d_{TBA-Cl} < 0.64$ nm. The origin ($z=0$, $r=0$) is located halfway between the centers of mass of TBA and Cl⁻. The vector connecting TBA and Cl⁻ is aligned along the *z* axis.
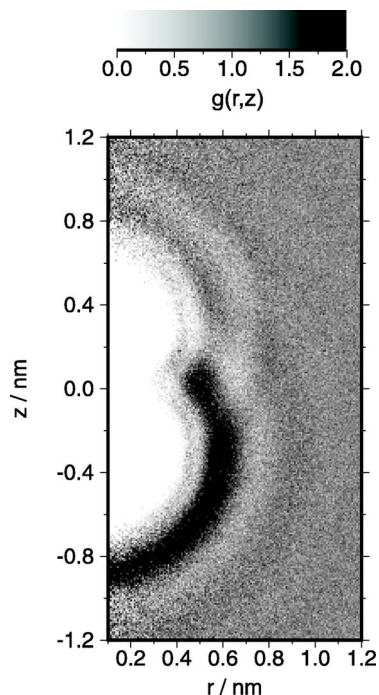
FIG. 7. Cylindrical pair distribution function TBA around a contact pair formed by a TBA molecule and a cloride ion (TBA:bottom; Cl⁻: top). The geometry and the definition of r and z are indicated in Fig. 6.

eral water properties somewhat better than SPC, such as OO-radial distribution functions,[78,79] the self-diffusion coefficients,[80] as well as the solvation entropy of small hydrophobic particles.[77] However, using their models for an aqueous salt solution, the preliminary data of Lee and van der Vegt indicated an association behavior of TBA very much similar to our MD simulations: An enhanced hydrophobic TBA-TBA association upon addition of sodium chloride.[81]

B. A combinatorial picture of TBA/water equilibrium in the chloride solvation shell

In this section we would like to elucidate the mechanism that determines the composition of the chloride solvation

shell by putting forward a simplified picture based on purely combinatorial arguments. This analysis will provide us also an estimate of the relative difference in binding free energy between TBA and water found in our MD simulation, as well as the one that would be necessary to create the Bowron-Finnney scenario of chloride-bridged TBA pairs.

First of all, we have statistically analyzed the structure of the first solvation shell of a chloride ion as it is provided by our MD simulations. We have calculated the probability P_n of finding a solvation shell with n TBA molecules. As members of the solvation shell are considered all TBA molecules with $r_{OH-Cl} \leqslant 0.39$ nm and all water molecules with $r_{OW-Cl} \leqslant 0.39$ nm (see Table IV and Fig. 2). These data are shown in the left part of Table V. Given are results for MD simulations at two different salt concentrations. Moreover, we also provide the average number of water molecules $\langle N_W \rangle_n$ in a solvation shell accommodating n TBA molecules.

The Cl–OW coordination number shown in Table IV, as well as the values for $\langle N_W \rangle_n$ given in Table V indicate that on average about seven to eight molecules (water and TBA) form the solvation shell of a chloride ion in the simulated solution. Now we would like to apply a simplified model of the solvation shell. Let us assume we have m sites (in our case, say, seven) in the shell that can be either occupied by water or a TBA molecule. Then the probability that a site is occupied by a TBA molecule is according to

$$p_T = \frac{K_{eq}N_T}{K_{eq}N_T + N_W}, \tag{15}$$

where N_T and N_W specify the number of TBA and water molecules in the simulation box, respectively. K_{eq} represents the constant describing the TBA/water equilibrium per solvation shell site. In fact, Eq. (15) represents the saturation limit for a Langmuir-type adsorption of a binary mixture (see Ref. 82, p. 80). Correspondingly, $\Delta G = -RT \ln K_{eq}$ represents the relative free energy change when replacing one water molecule by a TBA and might be considered as the difference in "binding strength." Given there are no further inter-site correlations within the solvation shell, the probability to find a chloride ion surrounded by exactly n TBA molecules

TABLE V. Statistical analysis of the composition of the first solvation shell of the solvated chloride ion. n specifies the number of TBA molecules in the solvation shell. P_n indicates the probability of finding a chloride ion with a solvation shell containing n TBA molecules. $\langle N_W \rangle_n$ indicates the average number of water molecules found in a solvation shell containing n TBA molecules. The left part of the table indicates the data obtained directly from the MD simulations. In the right part of the table the $P_n^{7(id)}(K_{eq})$ indicates the combinatorial prediction of the probability of finding a chloride ion with a solvation shell containing n TBA molecules (see text for details). Here K_{eq} is the equilibrium constant describing the *a priori* water/TBA equilibrium for each hydration shell site.

	MD simulation				Combinatorial prediction		
	2:100:1		2:100:2				
n	P_n	$\langle N_W \rangle_n$	P_n	$\langle N_W \rangle_n$	$P_n^{7(id)}(0.25)$	$p_n^{7(id)}(1)$	$P_n^{7(id)}(20)$
0	0.9677	6.94	0.9660	6.77	0.9657	0.8706	0.0948
1	0.0319	6.63	0.0335	6.48	0.0338	0.1219	0.2656
2	0.0004	6.37	0.0005	6.11	5.1×10^{-4}	7.3×10^{-3}	0.3187
3	0	⋯	0	⋯	4.2×10^{-6}	2.4×10^{-4}	0.2124
4	0	⋯	0	⋯	2.1×10^{-8}	4.9×10^{-6}	0.0850

follows a binomial distribution and is given by

$$P_n^{m(\mathrm{id})}(K_{\mathrm{eq}}) = \binom{m}{n} p_T^n (1 - p_T)^{(m-n)}. \qquad (16)$$

On the right hand side of Table V we illustrate three different cases: For the case of equal binding strength for water and TBA ($K_{\mathrm{eq}}=1$), the probabilities P_n are just determined by the composition of the solution (the N_T/N_W ratio). We would like to emphasize that even for this case the probability to find Cl-bridged dimers is below 1%. When comparing with the data obtained directly from the MD simulation, we find them well reproduced assuming $K_{\mathrm{eq}} \approx 0.25$. This indicates that a TBA molecule is on average more weakly bound to a chloride ion than a water molecule by about $\Delta G \approx 3.4$ kJ mol^{-1}. We would like to point out that due to the small value of $p_T \approx 5 \times 10^{-3}$, the obtained probabilities P_n depend only very weakly on the variation of the number of sites m (say, between 6 and 9) and are well approximated by a Poisson distribution. At last we would like to discuss a case, where the maximum in P_n is found for the case of Cl-bridged TBA dimers ($n=2$). To generate such a scenario, the equilibrium has to be shifted largely to the TBA side with $K_{\mathrm{eq}} \approx 20$, leading to a roughly 80 times stronger binding of TBA compared to our MD simulations, or an increase of about 11 kJ mol^{-1} on a free energy scale. Concluding, we would like to emphasize that unless the ion-TBA binding is not substantially stronger than the ion-water interaction, simply the vast majority of water molecules in the solution will prevent the formation of Cl-bridged TBA dimers. Finally, although our employed model potential is certainly far from being perfect, there is actually no indication on what could cause such a strong specific chloride-HO interaction. Moreover, the variation of the partial charges on the hydroxyl hydrogen (HO) varies only slightly among different force fields: +0.418$|e|$ for the all-atom OPLS model,[64] +0.423$|e|$ for Lee and van der Vegt's optimized united-atom OPLS model for TBA,[74] and +0.435$|e|$ for the united-atom TraPPE force field by Chen *et al.*[83] A specifically *linearly* chloride-bridged TBA pair would represent a state of additional configurational order and hence even lower entropy. Favoring this particular configuration among all others would therefore require an increasingly lower energy for this type of complex.

C. TBA clustering and "salting out"

To determine whether the observed enhanced hydrophobic aggregation upon addition of salt leads to a salting out of the TBA molecules, we present a cluster size analysis of the TBA aggregates. Such an approach has been recently put forward to study the onset of a demixing transition for the case of binary water-tetrahydrofuran mixtures[84] and to structurally characterize aqueous methanol solutions.[85] Based on the TBA-TBA central carbon pair correlation function (shown in Fig. 1) we consider two TBA molecules as "bound" when their CC-CC distance is smaller than 0.72 nm. We would like to point out that also hydrogen bonded TBA-TBA pairs are included by this definition. Based on that definition of intermolecular connectivity, we identify clusters of
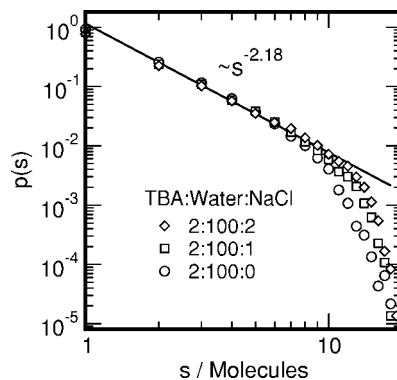

FIG. 8. Log-log plot of the probability $p(s)$ to find a TBA cluster of size s, where s indicates the number of TBA molecules in the cluster. The solid line indicates the behavior expected for random bond percolation on a 3D lattice close to the percolation transition (Ref. 86).

associated molecules. Figure 8 shows the log-log plot of the probability to find a cluster of a certain size s (number of TBA molecules) for the aqueous TBA solutions with increasing salt concentration. First of all, we would like to point out that for all shown distributions and for small cluster sizes, the distribution approaches $p(s) \sim s^{-\tau}$ with an exponent of $\tau \approx 2.18$, as observed for the case of random bond percolation on a three-dimensional (3D) lattice close to the percolation transition.[86] This seems to be well in accordance with the picture of an equilibrium of randomly associating and dissociating clusters of molecules. For larger cluster sizes, however, we observe a systematic deviation from the power-law behavior, which is due to the finite number of TBA molecules in our simulation. Please note that with increasing salt concentration an increased number of large clusters appears. This is a direct evidence for a "salting out" effect upon increased salt concentration. We would like to stress the observation that also by visual inspection the solutions still appear to be homogeneous and are apparently situated below a possible phase separation. Moreover, for a system close to a phase separation, we would expect the appearance of a "hump" at large cluster sizes. The relation of the buildup of such a narrow distribution of cluster sizes showing a maximum close to the largest possible cluster size (in our simulation: 20 TBA molecules) with the onset of phase separation has been recently demonstrated for the case of tetrahydrofuran/water mixtures by Oleinikova *et al.*[84]

However, we cannot fully rule out that the tendency of the system to phase separate might be also suppressed by finite size effects. To further substantiate the apparent salting out tendency, we show in Fig. 9 the distribution of cluster sizes of the largest cluster detected in each configuration. The maximum of each of the distribution functions is located in the vicinity of five molecules. However, there is a clear shift towards larger cluster sizes with increasing salt concentration. By promoting larger cluster sizes with increasing NaCl concentration, the TBA-clustering analysis clearly indicates a salting out tendency of the aqueous TBA solutions.

D. Self-diffusion coefficients

We have determined the self-diffusion coefficients for all particle types in the MD simulation from the mean square displacement according to
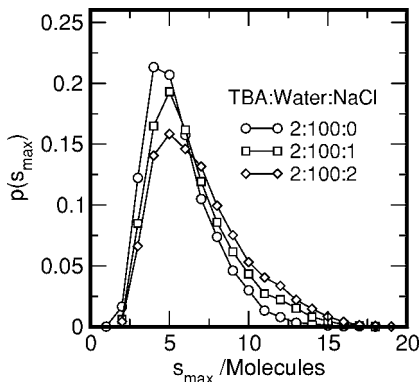
FIG. 9. Distribution of the size of the largest clusters s_{max} (number of TBA molecules) per configuration as a function of salt concentration.

$$D = \frac{1}{6} \lim_{t \to \infty} \frac{\partial}{\partial t} \langle |\mathbf{c}(t) - \mathbf{c}(0)|^2 \rangle, \qquad (17)$$

where $\mathbf{c}$ represents the position of the molecules' center of mass. In fact, the diffusion coefficients are obtained from the slope of the mean square displacement over the time interval between 100 and 500 ps. The lower boundary has been chosen to be large compared to the the average intermolecular association times. The diffusion coefficients obtained from the simulations are given in Table VI. In addition, the experimental self-diffusion coefficients for TBA-$d1$ in heavy water/salt solutions are shown in Table III.

It is evident that the experimental diffusion coefficients of TBA are substantially smaller than the values obtained from MD simulations. This has to be largely attributed to the fact that heavy water is used as a solvent in the experiment, which has a significantly smaller diffusion coefficient [$D = 1.768 \times 10^{-9}$ m^2 s^{-1} at 298.25 K (Ref. [87])] compared to H$_2$O [$D = 2.299 \times 10^{-9}$ m^2 s^{-1} at 298.2 K (Refs. [68] and [88])]. However, even when taking this effect into account, the diffusion coefficient of TBA according to the MD simulations seems to be overestimated by about 40%, which could indicate an increased number of associated TBA-TBA pairs in the experiment. This discrepancy may at least partly also be attributed to a possible enhanced "retardation effect"[89] of heavy water in the hydrophobic hydration shell of TBA. The retardation effect is clearly seen in the simulations as the slowing down of the water molecules in the TBA/water solution. However, given that the water retardation effect is related to the structuring of water in the hydrophobic hydra-

tion shell, it should rather be weaker in SPC/E than in real water, since SPC/E has been shown to underestimate the solvation entropy of hydrophobic particles.[77]

In addition, we find that the decrease of the TBA diffusion coefficient upon addition of salt by 6.4% / mol l^{-1} NaCl is significantly smaller than by the 15.8% / mol l^{-1} NaCl, as obtained in the MD simulation. The overestimated salt effect might be attributed to the potentially too small diffusion coefficients observed for Na$^+$ and particularly Cl$^-$. Scaling the ion self-diffusion coefficients with the diffusion coefficient of water in the TBA/water system (as approximation), one would expect diffusion coefficients of $D(\text{Na}^+) \approx 1.18 \times 10^{-9}$ m^2 s^{-1} and $D(\text{Cl}^-) \approx 1.70 \times 10^{-9}$ m^2 s^{-1} for the $c(\text{NaCl}) = 1.0$ mol l^{-1} concentration (using diffusion coefficients from Ref. [90] for the ions in aqueous solutions at the given concentration for 25 °C). Although the interaction with the TBA molecules might also have a non-negligible effect, the MD simulations seem to underestimate the self-diffusion coefficients of the ions by about 13% and 46%, respectively. To confirm this observation we have additionally calculated self-diffusion coefficients for a purely aqueous salt solution containing 500 SPC/E molecules and 16 ion pairs at 298 K and 1 bar, with a concentration of 1.67 mol. We obtain diffusion coefficients of $D(\text{Na}^+) = 1.07 \times 10^{-9}$ m^2 s^{-1}, $D(\text{Cl}^-) = 1.21 \times 10^{-9}$ m^2 s^{-1}, and $D(\text{H}_2\text{O}) = 2.18 \times 10^{-9}$ m^2 s^{-1}.

The diffusion coefficients of the ions clearly indicate that there is a need for improvement of the employed ion parameter sets. Particularly the hydration strength of the chloride ion seems to be overestimated by the present models. The overall agreement with the n-scattering data and the less satisfactory diffusion data, however, might just reflect the more pronounced sensitivity of kinetic quantities on details of the pair correlation function, such as the depth of the first minimum in the ion-water pair correlation function. This property is critically related to the water-exchange rate.

E. TBA-TBA association and the *A* parameter

Given the uncertainties associated with the use of empirical force field models, we have tried to find out whether there is also experimental evidence for an enhanced hydrophobic association scenario, as it is suggested by our MD simulations. Therefore we perform nuclear magnetic relaxation experiments on aqueous solutions of tertiary butanol

TABLE VI. Self-diffusion coefficients D_{self} as obtained from the MD simulations for the TBA/water and TBA/water/salt mixtures and for pure water. The star[*] indicates the parameter set for NaCl according to Koneshan *et al.* (Ref. [66].).

	D (10^{-9} m^2 s^{-1})				
			TBA:water:NaCl		
Particle	2:100:1[*]	2:100:2	2:100:1	2:100:0	0:100:0
H$_2$O	2.035±0.003	1.975±0.005	2.075±0.005	2.197±0.006	2.642±0.012
TBA	0.751±0.009	0.707±0.009	0.749±0.011	0.840±0.015	
Na$^+$	0.987±0.018	1.041±0.013	1.091±0.017		
Cl$^-$	1.200±0.021	1.162±0.014	1.290±0.020		

TABLE VII. Parameters characterizing the full H–H dipolar correlation function [according to Eq. (3)] for the TBA aliphatic hydrogen nuclei as obtained from the MD simulations. Given are both intra- and intermolecular contributions. The values are indicated by a 20% increased intermolecular relaxation rate $(T_1^{-1})_{inter}$ in the presence of NaCl, whereas the intramolecular rate changes only by about 2%. To obtain the correlation times τ_2 and prefactors $\langle r_{HH}^{-6}\rangle = G_2(0)$ [see Eq. (4)], the correlation function was integrated numerically while the tail of the correlation function was fitted to a single exponential function (inter: between 120 and 200 ps; intra: between 30 and 50 ps). The corresponding intra- and intermolecular relaxation times were finally obtained from Eq. (2).

TBA:water:NaCl	Inter-			Intra-		
	$\langle r_{HH}^{-6}\rangle$ (nm^{-6})	τ_2 (ps)	T_1 (s)	$\langle r_{HH}^{-6}\rangle$ (nm^{-6})	τ_2 (ps)	T_1 (s)
2:100	1667	8.89	79.0	76 920	4.41	3.45
2:100:1	1739	10.25	65.7	74 242	4.67	3.38
2:100:2	1958	10.61	56.3	74 239	4.85	3.25
2:100: 1*	1681	10.27	67.8	74 249	4.68	3.37

with varying salt concentration. Given a nonchanging intermolecular dipolar correlation time $\tau_{2,inter}$, an increasing relaxation rate of the methyl hydrogen nuclei would *directly* indicate an association behavior, as observed in our MD simulations. However, a decreasing relaxation rate would support the scenario obtained by Bowron and Finney. Since the correlation times are likely to be changing, we follow the *A*-parameter approach proposed by Hertz and co-workers, and discussed extensively in a previous section. The *A*-parameter approach is based on the assumption of a linear relationship between the intermolecular dipolar correlation time $\tau_{2,inter}$ and the inverse self-diffusion coefficient of the solute molecules [Eq. (9)], which can be both obtained independently. To prove this we have calculated the full inter- and intramolecular dipole-dipole correlation functions ac-

cording to Eq. (3) for the aliphatic hydrogens for all MD simulations, assuming all other protons to be exchanged by deuterons. Here only like-spin ^{1}H–^{1}H dipolar interactions are considered. A quantitative description of the intra- and intermolecular contributions as well as the calculated relaxation times T_1 are given in Table VII. The TBA self-diffusion coefficients for each of the simulated systems are given in Table VI. Figure 10(a) shows that the intermolecular correlation times $\tau_{2,inter}$ and the inverse self-diffusion coefficient of TBA are indeed almost linearly related, establishing the *A*-parameter approach as a valid approximation in the present case. Moreover, as Fig. 10(b) demonstrates, the *A* parameter from the MD data is also almost linearly related to the TBA-TBA coordination number, provoking an interpretation of the *A* parameter as an approximate direct measure of the TBA-TBA coordination number.

The *A* parameters obtained experimentally from the measured diffusion coefficients and relaxation rates are summarized in Table III. Both experimental and simulated *A* parameters are shown as well in Figure 11. MD simulation and experiment agree at least in a qualitative sense: with increasing salt concentration the rising *A* parameter indicates enhanced hydrophobic TBA-TBA aggregation. The quantitative difference of about 25% between the experimental and simulated *A* parameters might be partially attributed to imprecisions of the employed potential model, but might be
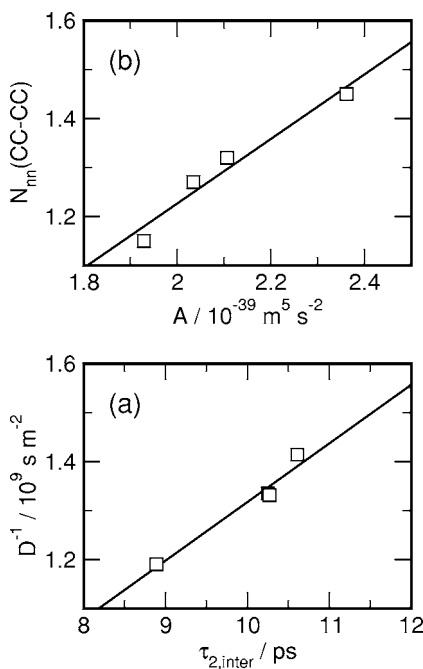

FIG. 10. *A*-parameter related quantities as obtained from the MD simulation: (a) inverse self-diffusion coefficient of TBA D^{-1} vs the intermolecular dipolar correlation time $\tau_{2,inter}$ of the aliphatic protons in TBA for the different MD simulations. (b) TBA-TBA aliphatic carbon coordination number vs the *A* parameter.
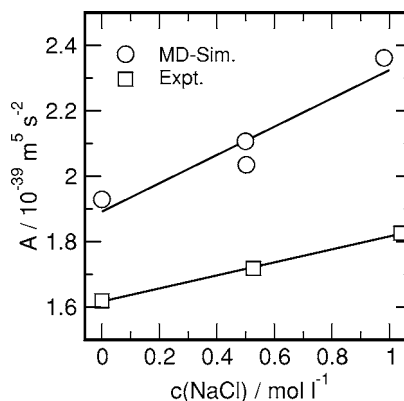

FIG. 11. *A* parameter obtained from MD simulation and experiment as a function of salt concentration.

based as well to a certain degree on the necessity for using D$_2$O as a solvent in the NMR measurements. Making use of the almost linear relationship between the *A* parameter and the TBA-TBA coordination number, we would finally like to determine approximate TBA-TBA coordination numbers for the NMR experimental data. Using Fig. 10(b), we get coordination numbers of N_{nn}(TBA)=0.975, 1.040, and 1.111 for the solutions with salt concentrations of 0.0, 0.5270, and 1.0403 mol l^{-1}, respectively. Although by about 25% smaller than the coordination numbers obtained from MD simulation, and suggesting a smaller concentration variation, the experimentally obtained *A* parameters and coordination numbers still tend to confirm an enhanced hydrophobic aggregation of the TBA molecules with increasing salt concentration. Finally, we would like to point out that these "experimental" coordination numbers are also in agreement with the error bars of the *n*-scattering data shown in Table IV.

IV. CONCLUSIONS

We have used a combination of molecular dynamics simulations and nuclear magnetic relaxation measurements to investigate the effect of salt (sodium chloride) on the association behavior of tertiary butanol molecules in an aqueous solution. We have shown that the application of the so-called *A*-parameter approach, proposed by Hertz and co-workers, employing solute-solute intermolecular ^1H-relaxation times and solute diffusion coefficients to determine the (relative) degree of association of solute molecules in aqueous solution, is well justified in the present case. Moreover, our MD simulations establish an almost linear relationship between the *A* parameter and the TBA-TBA coordination number.

Both MD simulations and NMR experiment tend to support a classical hydration and "salting out" picture of an enhanced tendency of forming hydrophobic contacts between the TBA molecules in the presence of salt. An increasing salt concentration is hence found to strengthen the solute-solute hydrophobic interaction. Consequently, also the TBA cluster-size distributions reveal a growing size of the TBA aggregates as the salt concentration increases and therefore show directly the "salting out" tendency. Apparently, the TBA molecules behave closely similar to purely hydrophobic solutes, as recently shown by Ghosh *et al.*[8] for the case of hydrophobic methane particles dissolved in aqueous salt solutions. In the light of the scenario recently suggested by Widom *et al.*[5] and Koga,[10] the salt thus would lead to an increase of the excess chemical potential of the hydrophobic groups (reduce their solubility) and would therefore provoke an enhanced aggregation. Based on lattice model calculations Widom *et al.* and Koga have proposed an almost inverse linear relationship between the excess chemical potential of hydrophobic solutes and their hydrophobic interaction strength.

Our detailed structural analysis of the simulation data does not provide any evidence for the presence of chloride-bridged butanol pairs, as proposed by Bowron and Finney.[23,26] Moreover, a combinatorial analysis of the composition of the chloride solvation shell reveals that the formation of a significant amount of dimers is probably just

prevented by the vast majority of water molecules in the solution. Finally, we would like to emphasize that although our results suggest a structurally completely distinct scenario, the molecular dynamics simulations, as well as the coordination numbers obtained indirectly from our NMR experimental data, appear to be largely within the experimental error bars of the *n*-scattering data of Bowron and Finney.[26]

[1] C. Tanford, *The Hydrophobic Effect: Formation of Micelles and Biological Membranes*, 2nd ed. (Wiley, New York, 1980).
[2] A. Ben-Naim, *Hydrophobic Interactions* (Plenum, New York, 1980).
[3] L. R. Pratt, Annu. Rev. Phys. Chem. **53**, 409 (2002).
[4] N. T. Southall, K. A. Dill, and A. D. J. Haymet, J. Phys. Chem. B **106**, 521 (2002).
[5] B. Widom, P. Bhimalapuram, and K. Koga, Phys. Chem. Chem. Phys. **5**, 3085 (2003).
[6] W. L. Masterton, D. Bolocofsky, and T. P. Lee, J. Phys. Chem. **75**, 2809 (1971).
[7] M. Kinoshita and F. Hirata, J. Chem. Phys. **106**, 5202 (1997).
[8] T. Ghosh, A. E. García, and S. Garde, J. Phys. Chem. B **107**, 612 (2003).
[9] T. Ghosh, A. Kalra, and S. Garde, J. Phys. Chem. B **109**, 642 (2005).
[10] K. Koga, J. Chem. Phys. **121**, 7304 (2004).
[11] D. Huang and D. Chandler, Proc. Natl. Acad. Sci. U.S.A. **97**, 8324 (2000).
[12] H. S. Ashbaugh and L. R. Pratt, e-print physics/0307109v2.
[13] S. Rajamani, T. M. Truskett, and S. Garde, Proc. Natl. Acad. Sci. U.S.A. **102**, 9475 (2005).
[14] D. Chandler, Nature (London) **437**, 640 (2005).
[15] M. Holz and M. Sörensen, Ber. Bunsenges. Phys. Chem. **96**, 1441 (1992).
[16] M. Holz, R. Grunder, A. Sacco, and A. Meleleo, J. Chem. Soc., Faraday Trans. **89**, 1215 (1993).
[17] A. Sacco, F. M. De Cillis, and M. Holz, J. Chem. Soc., Faraday Trans. **94**, 2089 (1998).
[18] M. Mayele, M. Holz, and A. Sacco, Phys. Chem. Chem. Phys. **1**, 4615 (1999).
[19] M. Mayele and M. Holz, Phys. Chem. Chem. Phys. **2**, 2429 (2000).
[20] G. W. Euliss and C. M. Sorensen, J. Chem. Phys. **80**, 4767 (1984).
[21] D. T. Bowron, J. L. Finney, and A. K. Soper, J. Phys. Chem. B **102**, 3551 (1998).
[22] D. T. Bowron, A. K. Soper, and J. L. Finney, J. Chem. Phys. **114**, 6203 (2001).
[23] D. T. Bowron and J. L. Finney, Phys. Rev. Lett. **89**, 215508 (2002).
[24] S. Dixit, J. Crain, W. C. K. Poon, J. L. Finney, and A. K. Soper, Nature (London) **416**, 829 (2002).
[25] D. T. Bowron and S. Díaz Moreno, J. Chem. Phys. **117**, 3753 (2002).
[26] D. T. Bowron and J. L. Finney, J. Chem. Phys. **118**, 8357 (2003).
[27] M. G. Cacace, E. M. Landau, and J. J. Ramsden, Q. Rev. Biophys. **30**, 241 (1997).
[28] F. Hofmeister, Arch. Exp. Path. und Pharmakol. (Leipzig) **24**, 247 (1888) [Curr. Opin. Colloid Interface Sci. **9**, 19 (2004)].
[29] V. A. Parsegian, Nature (London) **378**, 335 (1995).
[30] B. Hribar, N. T. Southall, V. Vlachy, and K. A. Dill, J. Am. Chem. Soc. **124**, 12302 (2002).
[31] A. Geiger, Ber. Bunsenges. Phys. Chem. **85**, 52 (1981).
[32] R. Leberman and A. K. Soper, Nature (London) **378**, 364 (1995).
[33] J. L. Finney and A. K. Soper, Chem. Soc. Rev. **23**, 1 (1994).
[34] A. K. Soper, Chem. Phys. **202**, 295 (1996).
[35] A. K. Soper, Mol. Phys. **99**, 1503 (2001).
[36] D. T. Bowron, Philos. Trans. R. Soc. London, Ser. B **359**, 1167 (2004).
[37] J. L. Finney and D. T. Bowron, Curr. Opin. Colloid Interface Sci. **9**, 59 (2004).
[38] J. L. Finney and D. T. Bowron, Philos. Trans. R. Soc. London, Ser. A

363, 469 (2004).

[39] M. G. Burke, R. Woscholski, and S. N. Yaliraki, Proc. Natl. Acad. Sci. U.S.A. **100**, 13928 (2003).

[40] H. G. Hertz, Prog. Nucl. Magn. Reson. Spectrosc. **3**, 159 (1967).

[41] H. G. Hertz and R. Tutsch, Ber. Bunsenges. Phys. Chem. **80**, 1268 (1976).

[42] A. Abragam, *The Principles of Nuclear Magnetism* (Oxford University Press, Oxford, 1961).

[43] P. Westlund and R. Lynden-Bell, J. Magn. Reson. (1969-1992) (1969–1992) **72**, 522 (1987).

[44] M. Odelius, A. Laaksonen, M. H. Levitt, and J. Kowalewski, J. Magn. Reson., Ser. A **105**, 289 (1993).

[45] E. O. Stejksal, D. E. Woessner, T. C. Farrar, and H. S. Gutowsky, J. Chem. Phys. **31**, 55 (1959).

[46] P. A. Egelstaff, *An Introduction to the Liquid State*, 2nd ed. (Oxford University Press, Oxford, 1992).

[47] A. L. Capparelli, H. G. Hertz, and R. Tutsch, J. Phys. Chem. **82**, 2023 (1978).

[48] K. J. Müller and H. G. Hertz, J. Phys. Chem. **100**, 1256 (1996).

[49] W. S. Price, Concepts Magn. Reson. **10**, 197 (1998).

[50] U. Wandle and H. G. Hertz, Z. Phys. Chem. **178**, 217 (1992).

[51] S. Nosé, Mol. Phys. **52**, 255 (1984).

[52] W. G. Hoover, Phys. Rev. A **31**, 1695 (1985).

[53] M. Parrinello and A. Rahman, J. Appl. Phys. **52**, 7182 (1981).

[54] S. Nosé and M. L. Klein, Mol. Phys. **50**, 1055 (1983).

[55] U. Essmann, L. Perera, M. L. Berkowitz, T. A. Darden, H. Lee, and L. G. Pedersen, J. Chem. Phys. **103**, 8577 (1995).

[56] S. Miyamoto and P. A. Kollman, J. Comput. Chem. **13**, 952 (1992).

[57] J. P. Ryckaert, G. Ciccotti, and H. J. C. Berendsen, J. Comput. Phys. **23**, 327 (1977).

[58] E. Lindahl, B. Hess, and D. van der Spoel, J. Mol. Model. **7**, 306 (2001).

[59] D. van der Spoel, E. Lindahl, B. Hess *et al.*, GROMACS User Manual, version 3.2, 2004; www.gromacs.org.

[60] D. Paschek, MOSCITO4 molecular dynamics simulation package (2005); www.moscitomd.de.

[61] H. Flyvbjerg and H. G. Petersen, J. Chem. Phys. **91**, 461 (1989).

[62] H. J. C. Berendsen, J. P. M. Postma, W. F. van Gunsteren, A. DiNola, and J. R. Haak, J. Chem. Phys. **81**, 3684 (1984).

[63] H. J. C. Berendsen, J. R. Grigera, and T. P. Straatsma, J. Phys. Chem. **91**, 6269 (1987).

[64] W. L. Jorgensen, D. S. Maxwell, and J. Tirado-Rives, J. Am. Chem. Soc. **118**, 11225 (1996).

[65] K. Heinzinger, in *Computer Modelling of Fluids Polymers and Solids*, NATO ASI Series Vol. C293, edited by C. R. A. Catlow, S. C. Parker, and M. P. Allen (Kluwer Academic Publishers, Dordrecht, 1990), pp. 357–369.

[66] S. Koneshan, J. C. Rasaiah, R. M. Lynden-Bell, and S. H. Lee, J. Phys. Chem. B **102**, 4193 (1998).

[67] G. Bonera and A. Rigamonti, J. Chem. Phys. **42**, 171 (1965).

[68] R. Mills, J. Chem. Phys. **77**, 685 (1973).

[69] E. M. Knipping, M. J. Lakin, K. L. Foster, P. Jungwirth, D. J. Tobias, R. B. Gerber, D. Dabdub, and B. J. Finlayson-Pitts, Science **288**, 301 (2000).

[70] P. Jungwirth and D. J. Tobias, J. Phys. Chem. B **104**, 7702 (2000).

[71] P. Jungwirth and D. J. Tobias, J. Phys. Chem. B **105**, 10468 (2001).

[72] H. A. Patel, E. B. Naumann, and S. Garde, J. Chem. Phys. **119**, 9199 (2003).

[73] I. Brovchenko, A. Geiger, and A. Oleinikova, J. Phys.: Condens. Matter **16**, S5345 (2004).

[74] M. E. Lee and N. F. A. van der Vegt, J. Chem. Phys. **122**, 114509 (2005).

[75] H. J. C. Berendsen, J. P. M. Postma, W. F. van Gunsteren, and J. Hermans, in *Intermolecular Forces*, edited by B. Pullmann (Reidel, Dordrecht, 1981), pp. 331–338.

[76] W. L. Jorgensen, J. Phys. Chem. **90**, 1276 (1986).

[77] D. Paschek, J. Chem. Phys. **120**, 6674 (2004).

[78] G. Hura, J. M. Sorenson, R. M. Glaeser, and T. Head-Gordon, J. Chem. Phys. **113**, 9140 (2000).

[79] J. M. Sorenson, G. Hura, R. M. Glaeser, and T. Head-Gordon, J. Chem. Phys. **113**, 9149 (2000).

[80] D. van der Spoel, P. J. van Maaren, and H. J. C. Berendsen, J. Chem. Phys. **108**, 10220 (1998).

[81] N. F. A. van der Vegt (private communication).

[82] A. Ben-Naim, *Statistical Thermodynamics for Chemists and Biochemists* (Plenum, New York, 1992).

[83] B. Chen, J. J. Potoff, and J. I. Siepmann, J. Phys. Chem. B **105**, 3093 (2001).

[84] A. Oleinikova, I. Brovchenko, A. Geiger, and B. Guillot, J. Chem. Phys. **117**, 3296 (2002).

[85] L. Dougan, S. P. Bates, R. Hargreaves, J. P. Fox, J. Crain, J. L. Finney, V. Réat, and A. K. Soper, J. Chem. Phys. **121**, 6465 (2004).

[86] D. Stauffer and A. Aharony, *Introduction to Percolation Theory*, 2nd ed. (CRC, Boca Raton, FL, 1994).

[87] W. S. Price, H. Ide, Y. Arata, and O. Söderman, J. Phys. Chem. B **104**, 5874 (2000).

[88] M. Holz, S. R. Heil, and A. Sacco, Phys. Chem. Chem. Phys. **2**, 4740 (2000).

[89] R. Haselmeier, M. Holz, W. Marbach, and H. Weingärtner, J. Phys. Chem. **99**, 2243 (1995).

[90] R. Mills and V. M. M. Lobo, *Self-diffusion in Electrolyte Solutions*, Physical Sciences Data Vol. 36 (Elsevier, Amsterdam, The Netherlands, 1989).